Robust Identification with Mixed Parametric/Nonparametric Models and Time/Frequency-Domain Experiments: Theory and an Application

Tamer Inanc, Mario Sznaier, *Member, IEEE*, Pablo A. Parrilo, and Ricardo S. Sánchez Peña, *Senior Member, IEEE*

***Abstract*—We have recently proposed a new robust identification framework, based upon generalized interpolation theory, that allows for combining parametric and nonparametric models and frequency and time-domain experimental data. In this paper we illustrate the advantages of this framework over conventional control oriented identification techniques by considering the problem of identifying a two-degree of freedom structure used as a testbed for demonstrating damage-mitigation and life extension control concepts. This structure is lightly damped, leading to time and frequency domain responses that exhibit large peaks, thus rendering the identification problem nontrivial.**

***Index Terms*—Convex optimization, Carathéodory–Fejér problem, interpolatory algorithms, Nevanlinna–Pick interpolation, robust identification.**

I. Introduction

During the past few years a large research effort has been devoted to the problem of developing deterministic identification procedures that, starting from experimental data and an *a priori* class of models, generate a nominal model and bounds on identification errors. These models and bounds can then be combined with standard robust control synthesis methods (such as $\mathcal{H}_\infty$, μ or ℓ^1) to obtain robust systems. This problem, termed the robust identification problem was originally posed by Helmicki *et al.* [6] and has since attracted considerable attention. Depending on whether the experimental data available originates from frequency or time-domain experiments, this framework leads to $\mathcal{H}_\infty$ [1], [5], [6], [14] or ℓ_1-based identification [7], [9], [10], respectively. Interpolatory algorithms exploiting both sources of data have been proposed in [3], [17], [11].

However, a potential drawback of these methods is their nonparametric nature. In many cases, part of the model has a clear parametric structure, and disregarding this information may lead to very conservative results. A typical case is the identification of a lightly damped flexible structures, where the use of nonparametric methods leads to high-order models in order to capture the frequency response around sharp resonance peaks. In this situation, a good time-domain fit can be obtained using the methods proposed in [4] and [8]. However, since these methods are based on time-domain data, they do not guarantee good frequency domain fitting. In addition, they do not allow for incorporating a nonparametric part to take into account unmodeled dynamics.

Finally, in [13] we have recently proposed a framework that allows for combining parametric and nonparametric models in the context of mixed frequency/time-domain robust identification. In this paper, we briefly review this framework and we illustrate its advantages by considering the problem of identifying a model of a two-degree of freedom structure. This structure, used as a testbed for life-extending controllers [16], has a very lightly damped resonant mode, resulting in a nontrivial identification problem. As we show in the paper, conventional single objective robust identification tools (either ℓ^1 or $\mathcal{H}_\infty$) fail to capture the complete behavior of the plant. On the other hand, nonparametric mixed identification yields acceptable results, at the price of large order models. This difficulty can be overcome by modeling the low-frequency behavior of the plant using second-order Kautz filters. The parametric portion of the framework is used to identify the parameters of these filters, while nonparametric identification is used for the remaining (mostly high-frequency) portion. As shown in Section IV this results in low-order models that capture both the time and frequency domain behavior of the plant. Moreover, this is achieved using the same total number of experimental data points, hence similar computational complexity, as in the conventional single objective identification.

Manuscript received February 28, 2000. Manuscript received in final form November 20, 2000. Recommended by Associate Editor C. Knospe. This work was supported in part by NSF under Grants ECS-9625920 and ECS-9907051.

T. Inanc and M. Sznaier are with the Department of Electrical Engineering, Penn State University, University Park, PA 16802 USA.

P. A. Parrilo is with the Department of Control and Dynamical Systems, Caltech, Pasadena, CA 91125 USA.

R. S. Sánchez Peña is with the National Commission of Space Activities (CONAE), Argentina.

Publisher Item Identifier S 1063-6536(01)03360-7.

II. Preliminaries

A. Notation

$\mathcal{H}_\infty$ denotes the space of complex functions with bounded analytic continuation inside the unit disk, equipped with the norm $\|G(z)\|_\infty \triangleq ess\ \sup_{|z|<1} \overline{\sigma}(G(z))$. Also of interest is the space $\mathcal{H}_{\infty,\rho}$ of transfer matrices in $\mathcal{H}_\infty$ which have analytic continuation inside the disk of radius $\rho > 1$, i.e., the space of exponentially stable systems with a stability margin of $(\rho - 1)$, equipped with the norm $\|G(z)\|_{\infty,\rho} \triangleq \sup_{|z|<\rho} \overline{\sigma}(G(z))$.

ℓ_1 denotes the space of absolutely summable sequences $h = \{h_i\}$ equipped with the norm $\|h\|_{\ell_1} \triangleq \sum_{i=0}^{\infty} |h_i| < \infty$. Similarly ℓ_∞ denotes the space of bounded sequences $h = \{h_i\}$ equipped with the norm $\|h\|_{\ell_\infty} \triangleq \sup_{i\geq 0} |h_i| < \infty$. Given a sequence $h \in \ell_1$, its z-transform is defined as $H(z) = \sum_{i=0}^{\infty} h_i z^i$.

For simplicity in the sequel we consider single input–single output (SISO) models, although all results can be applied to multiple input–multiple output (MIMO) systems, following Chen *et al.* [2].

B. The Robust Identification Framework

In this paper we consider the case where the *a posteriori* experimental data originates from two different sources: 1) frequency and 2) time domain experiments. The first type of information consists of a set of N_f samples of the frequency response of the system: $y_k^f = \hat{h}_k + \eta_k^f$, $k = 0, \ldots, N_f - 1$, where $\hat{h}_k = H(e^{j\Omega_k})$, $k = 0, \ldots, N_f - 1$, Ω_k denotes the sampling frequencies; and where η_k^f represents complex additive noise, bounded by ϵ_f in the ℓ_∞ norm.

The time domain data consists of a set of the first N_t samples of the time response corresponding to a known but otherwise arbitrary input, also corrupted by additive noise $y_n^t = (Uh)_n + \eta_n^t$, $n = 0, \ldots, N_t - 1$, where

$$U = \begin{bmatrix} u_0 & 0 & \ldots & 0 \\ u_1 & u_0 & \ldots & 0 \\ \vdots & \ddots & \ddots & 0 \\ u_{N_t-1} & \ldots & u_1 & u_0 \end{bmatrix}$$

is the Toeplitz matrix corresponding to the input sequence and where the noise η_n^t is real and satisfies $\|\eta^t\|_{\ell_\infty} \leq \epsilon_t$. In the sequel, for notational simplicity we will collect the samples y_k^f and y_n^t in the vectors $\mathbf{y}^f \in \mathbb{C}^{N_f}$ and $\mathbf{y}^t \in \mathcal{R}^{N_t}$.

The *a priori* information available is that the system H under consideration belongs to the following classes of models:

1) $H(z) = G_p(z) + G_{np}(z)$ where G_p and G_{np} denote the parametric and nonparametric part, respectively.
2) The parametric portion $G_p(z)$ belongs to the following class $\mathcal{P}$ of affine models:

$$\mathcal{P} \triangleq \{\mathbf{p}^T \mathbf{G}(z),\ \mathbf{p} \in \mathcal{R}^{N_p},\ p_i \in [a_i,\ b_i]\}$$

   where the components $G_i(z)$ of vector $\mathbf{G}(z)$ are known functions.
3) The nonparametric portion G_{np} belongs to the class of models $\mathcal{S} \triangleq \Phi \cap \mathcal{H}_\infty(\rho,\ K)$ where
   a) $\mathcal{H}_\infty(\rho,\ K) \triangleq \{G_{np}(z) \in \mathcal{H}_{\infty,\rho}\colon \|G_{np}\|_{\infty,\rho} < K\}$
   b) Φ is the set of models satisfying a time-domain bound of the form: $\Phi \triangleq \{g(\cdot) | \phi_\ell(k) \leq g(k) \leq \phi_u(k),\ k = 0,\ N_\phi - 1\}$

To recap, the *a priori* information and the *a posteriori* experimental input data are

$$\begin{aligned} \mathcal{T} &= \{H(z) = G_p(z) + G_{np}(z) \,|\, G_p \in \mathcal{P},\ G_{np}(z) \in \mathcal{S}\} \\ \mathcal{N}_f &= \ell_\infty(\epsilon_f) = \left\{\eta^f \in \mathbb{C}^{N_f},\ |\eta_k^f| < \epsilon_f\right\} \\ \mathcal{N}_t &= \ell_\infty(\epsilon_t) = \{\eta^t \in \mathcal{R}^{N_t},\ |\eta_k^t| < \epsilon_t\} \\ \mathbf{y}^f &= \left\{\hat{h} + \eta^f \in \mathbb{C}^{N_f}\right\} \\ \mathbf{y}^t &= \left\{[(Uh)_j + \eta_j^t]_{0,\ N_t-1} \in \mathcal{R}^{N_t}\right\}. \end{aligned} \tag{1}$$

By using these definitions the robust identification problem with mixed models and data can be precisely stated as the following.

Problem 1: Given the experiments $(\mathbf{y}^f,\ \mathbf{y}^t)$ and the *a priori* sets $(\mathcal{T},\ \mathcal{N}_f,\ \mathcal{N}_t)$, determine:

1) if the *a priori* and *a posteriori* information are consistent, i.e., the consistency set

$$\mathcal{T}(\mathbf{y}^f,\ \mathbf{y}^t) \triangleq \left\{ H \in \mathcal{T} \,\middle|\, \begin{matrix} (\mathbf{y}^f - \hat{h}) \in \mathcal{N}_f \\ (\mathbf{y}^t - Uh) \in \mathcal{N}_t \end{matrix} \right\} \tag{2}$$

   is nonempty;
2) a nominal model which belongs to the consistency set $\mathcal{T}(\mathbf{y}^f,\ \mathbf{y}^t)$;
3) a bound on the worst case identification error.

Next we recall a result from [13] showing consistency can be established by solving an LMI feasibility problem.

Theorem 1: Define

$$P_t = \begin{bmatrix} g_1(0) & g_2(0) & \ldots & g_{N_p}(0) \\ g_1(1) & g_2(1) & \ldots & g_{N_p}(1) \\ \vdots & \vdots & \ddots & \vdots \\ g_1(N_t-1) & g_2(N_t-1) & \ldots & g_{N_p}(N_t-1) \end{bmatrix} \tag{3}$$

and

$$P_f = \begin{bmatrix} G_1(z_0) & G_2(z_0) & \ldots & G_{N_p}(z_0) \\ G_1(z_1) & G_2(z_1) & \ldots & G_{N_p}(z_1) \\ \vdots & \vdots & \ddots & \vdots \\ G_1(z_{N_f-1}) & G_2(z_{N_f-1}) & \ldots & G_{N_p}(z_{N_f-1}) \end{bmatrix}. \tag{4}$$

Then, the *a priori* and *a posteriori* information are consistent if and only if there exists three vectors

$$\mathbf{p} = \begin{bmatrix} p_1 \\ p_2 \\ \ldots \\ p_{N_p} \end{bmatrix}, \qquad \mathbf{w} = \begin{bmatrix} w_0 \\ w_1 \\ \ldots \\ w_{N_f-1} \end{bmatrix}, \qquad \mathbf{h} = \begin{bmatrix} h_0 \\ h_1 \\ \ldots \\ h_{N_t-1} \end{bmatrix} \tag{5}$$

such that

$$Z(\mathbf{w},\ \mathbf{h}) > 0 \tag{6}$$

$$(\mathbf{y}^f - P_f\mathbf{p} - \mathbf{w}) \in \mathcal{N}_f \tag{7}$$

$$(\mathbf{y}^t - UP_t\mathbf{p} - U\mathbf{h}) \in \mathcal{N}_t \tag{8}$$

where

$$
\begin{aligned}
Z &= \begin{bmatrix} M_0^{-1} & \frac{1}{K}X \\ \frac{1}{K}X^* & M_0 \end{bmatrix} \\
M_0 &= \begin{bmatrix} Q & S_0R^{-2} \\ R^{-2}S_0^* & R^{-2} \end{bmatrix} \\
X &= \begin{bmatrix} \mathcal{W}_f & 0 \\ 0 & \mathcal{F}_t \end{bmatrix} \\
R &= \operatorname{diag}\begin{bmatrix} 1 & \rho & \rho^2 & \cdots \rho^{N_t-1} \end{bmatrix} \\
Q &= \left[\frac{\rho^2}{\rho^2 - z_i z_j}\right]_{ij} \\
S_0 &= \begin{bmatrix} 1 & \overline{z}_0 & \overline{z}_0^2 & \cdots & \overline{z}_0^{N_t-1} \\ 1 & \overline{z}_1 & \overline{z}_1^2 & \cdots & \overline{z}_1^{N_t-1} \\ \vdots & \vdots & \vdots & \vdots & \vdots \\ 1 & \overline{z}_{N_f-1} & \overline{z}_{N_f-1}^2 & \cdots & \overline{z}_{N_f-1}^{N_t-1} \end{bmatrix} \\
\mathcal{W}_f &= \operatorname{diag}\begin{bmatrix} w_0 & \cdots & w_{N_f-1} \end{bmatrix} \\
\mathcal{F}_t &= \begin{bmatrix} h_0 & h_1 & \cdots & h_{N_t-1} \\ 0 & h_0 & \cdots & h_{N_t-2} \\ \vdots & \vdots & \ddots & \vdots \\ 0 & 0 & \cdots & h_0 \end{bmatrix}.
\end{aligned} \tag{9, 10}
$$

C. Identification

Once consistency is established, the second step toward solving Problem 1 consists of generating a nominal model in the consistency set $\mathcal{T}(\mathbf{y}^f, \mathbf{y}^t)$, proceeding as follows.

1) Find feasible data vectors $\mathbf{p}$, $\mathbf{w}$, $\mathbf{h}$ for the consistency problem by solving the LMI feasibility problem given by (6)–(8).
2) Compute a model from the consistency set $\mathcal{S}$ for the nonparametric portion of the plant. Recall that all the models in $\mathcal{S}$ can be parameterized as a linear fractional transformation (LFT) of a free parameter $q(z) \in \mathcal{H}_\infty, \|q\|_\infty \leq 1$, as follows:

$$G_{np}(z) = F_\ell[L(z), q(z)] \tag{11}$$

$$L(z) = \begin{bmatrix} T_{12}T_{22}^{-1} & T_{11} - T_{12}T_{22}^{-1}T_{21} \\ T_{22}^{-1} & -T_{22}^{-1}T_{21} \end{bmatrix} \tag{12}$$

where the transfer function $T(z)$ depends on the experimental data and the solution to the LMI problem (see [11] for details).

Since the proposed algorithm is interpolatory, it has several advantages over the usual "two step" algorithms sometimes used in the context of robust identification [5], [6]. In particular, since the identified model is in set $\mathcal{S}(\mathbf{y}^f, \mathbf{y}^t)$, its distance to the Chebyshev center of this set is within the diameter of information. As a consequence the algorithm is optimal up to a factor of two as compared with central strongly optimal procedures. For the same reasons, it is also convergent and therefore the modeling error tends to zero as the information is completed.

D. Some Numerical Considerations

From Theorem 1 we have that the central [i.e., $q(z) = 0$] nonparametric identified model is given by

$$G_{np}(z) = T_{12}T_{22}^{-1}. \tag{13}$$

Note however that since T_{12} and T_{22} have the same poles, attempting to compute $G_{np}(z)$ from (13) will lead to a large number of quasi pole/zero cancellations and numerical difficulties. To avoid these difficulties we will compute $G_{np}(z)$ explicitly. As a byproduct of this computation we will show that there exists $N_t + N_f$ exact pole/zero cancellations in (13). To this effect start by rewriting T_{12} and T_{22} in Theorem 1 explicitly as

$$T_{12} = \left[\begin{array}{c|c} A_T & B_2 \\ \hline C_1 & D_{12} \end{array}\right], \qquad T_{22} = \left[\begin{array}{c|c} A_T & B_2 \\ \hline C_2 & D_{22} \end{array}\right] \tag{14}$$

where

$$B_2 = M_R^{-1}(A_T^* - I)^{-1}C_-^* \tag{15}$$

$$C_1 = C_+(A_T - I) \tag{16}$$

$$C_2 = C_-(A_T - I) \tag{17}$$

$$D_{12} = C_+M_R^{-1}(A_T^* - I)^{-1}C_-^* \tag{18}$$

$$D_{22} = 1 + C_-M_R^{-1}(A_T^* - I)^{-1}C_-^*. \tag{19}$$

Straightforward calculations show that

$$
\begin{aligned}
G_{np}(z) &= T_{12}T_{22}^{-1} \\
&= \left[\begin{array}{cc|c} A_T - B_2D_{22}^{-1}C_2 & 0 & -B_2D_{22}^{-1} \\ B_2D_{22}^{-1}C_2 & A_T & B_2D_{22}^{-1} \\ \hline D_{12}D_{22}^{-1}C_2 & C_1 & D_{12}D_{22}^{-1} \end{array}\right].
\end{aligned} \tag{20}
$$

Using the similarity transformation $T = \left[\begin{smallmatrix} I & 0 \\ -I & I \end{smallmatrix}\right]$ and removing uncontrollable and unobservable modes yields

$$G_{np}(z) = \left[\begin{array}{c|c} A_T - B_2D_{22}^{-1}C_2 & -B_2D_{22}^{-1} \\ \hline D_{12}D_{22}^{-1}C_2 - C_1 & D_{12}D_{22}^{-1} \end{array}\right]. \tag{21}$$

Finally, using the matrix inversion lemma to compute D_{22}^{-1} explicitly yields the following expression for $G_{np}(z)$:

$$G_{np}(z) = \left[\begin{array}{c|c} G_{11} & G_{12} \\ \hline G_{21} & G_{22} \end{array}\right] \tag{22}$$

$$
\begin{aligned}
G_{11} &= A_T - [C_-^*C_- + (A_T^* - I)M_R]^{-1} \\
&\quad \cdot C_-^*C_-(A_T - I)
\end{aligned} \tag{23}
$$

$$G_{12} = -[(A_T^* - I)M_R + C_-^*C_-]^{-1}C_- \tag{24}$$

$$
\begin{aligned}
G_{21} &= C_+[(A_T^* - I)M_R + C_-^*C_-]^{-1}C_-^*C_-(A_T - I) \\
&\quad - C_+(A_T - I)
\end{aligned} \tag{25}
$$

$$G_{22} = C_+[(A_T^* - I)M_R + C_-^*C_-]^{-1}C_-^* \tag{26}$$

TABLE I
DESCRIPTION OF THE TESTBED

Masses: $M_1 = 2.702$ lbm	$M_2 = 7.664$ lbm		
Beam 1: $L_1 = 8.5$in.	$H_1 = 0.122$ in.	$W_1 = 0.437$ in.	$E_1 = 10.5 \times 10^6$ psi
Beam 2: $L_2 = 11.84$ in.	$H_2 = 0.437$ in.	$W_2 = 0.87$ in.	$E_2 = 30 \times 10^6$ psi.
Sampling frequency: $f_s = 46.5$ Hz	($T_s = 21.5$ msec.)		
LDVT: Trans-tek 0243			
Data Acquisition: Keithley DAS–1600,	12 bit resolution		

Practical implementation of the algorithm also requires addressing the issue of the conditioning of the problem as the cardinality of the data grows. Note that reducing the consistency problem to an LMI feasibility problem required an explicit inversion of M_0. However, while this matrix M_0 is always positive definite, is asymptotically singular, with its condition number growing without bound as the number of data points increases. The following lemma gives an estimate on the growth of M_0's condition number in the most favorable case, i.e., when the z_i are equidistant[1] (roots of the unity). It provides a lower bound on the conditioning of matrix M_0.

Lemma 1: Let $z_k = e^{j(2\pi k/N_f)}$, $k = 0, \ldots, N_f - 1$ (the N_fth roots of the unity). In this case, the singular values and condition number of M_0 (Nevanlinna–Pick) are bounded by

$$\sigma_1(M_0) \geq \sigma_i(Q) = \frac{1}{\rho^i}\frac{N_f\rho^{N_f}}{\rho^{N_f}-1} \geq \sigma_{N_f}(M_0), \quad i = 1, \ldots, N_f \tag{27}$$

$$\kappa(M_0) \geq \kappa(Q) = \frac{\sigma_1(Q)}{\sigma_{N_f}(Q)} = \rho^{N_f-1}. \tag{28}$$

Proof: When the z_k are chosen as the roots of unity, the Pick matrix is a *circulant* matrix, i.e., $Q_{ij} = c_{(i-j) \bmod N_t}$. Since Q is normal, its singular values are the absolute value of its eigenvalues. Since the eigenvalues of a circulant matrix can be obtained as the discrete Fourier transform of the elements of the first row, it follows that the singular values of Q can be obtained from the following equality[2]:

$$\sum_{k=0}^{N_f-1} \frac{e^{j(2\pi/N_f)kl}}{\rho - e^{j(2\pi/N_f)k}} = \frac{N_f\rho^{N_f-1-l}}{\rho^{N_f}-1}.$$

The desired result follows now from the interlacing property of the eigenvalues of a symmetric matrix and its diagonal submatrix (Q in this case). □

Thus, we see that the condition number of the generalized Pick matrix, has at least an exponential growth with the number of frequency data samples.

III. APPLICATION: ROBUST IDENTIFICATION OF A FLEXIBLE STRUCTURE

In this section, we illustrate the proposed framework by applying it to the problem of identifying a flexible structure. This mass-beam system, intended to model a plant subjected

[1]If for some i, j, $|z_i - z_j| < \epsilon$, as $\epsilon \to 0$, M_0 tends to singularity.

[2]This equality follows from considering the partial fraction expansion of the right-hand side (as a function of ρ).

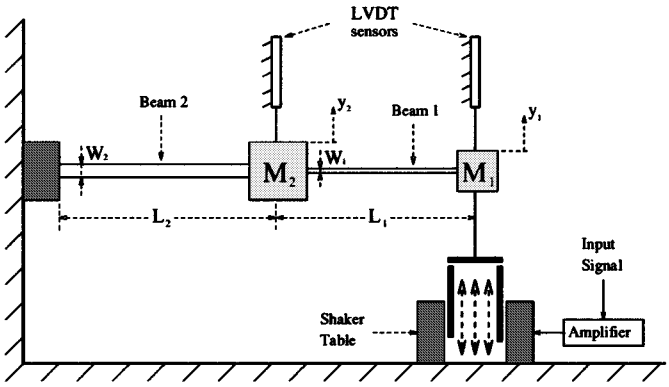

Fig. 1. The flexible testbed.

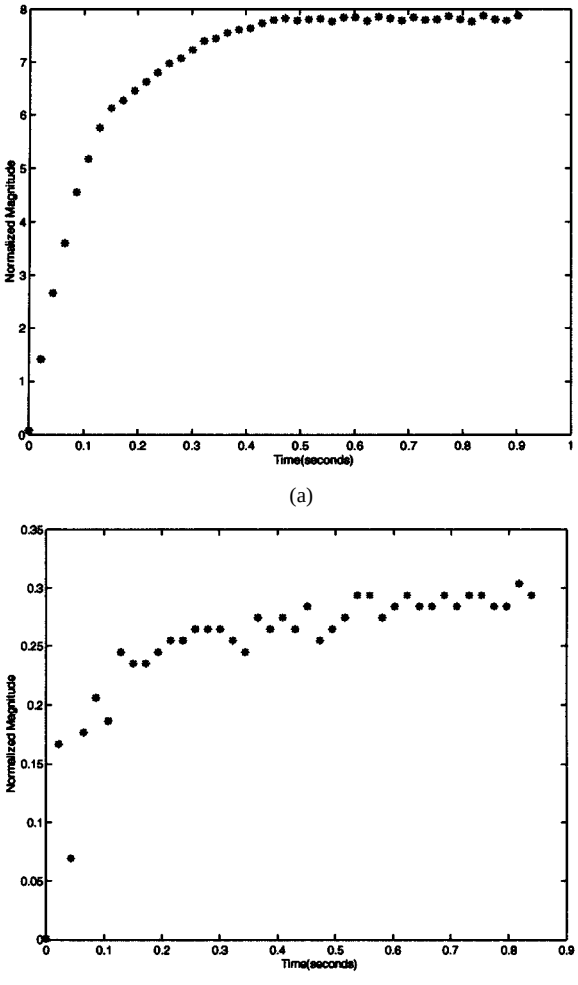

Fig. 2. Normalized experimental time-domain data points (a) y_1 and (b) y_2.

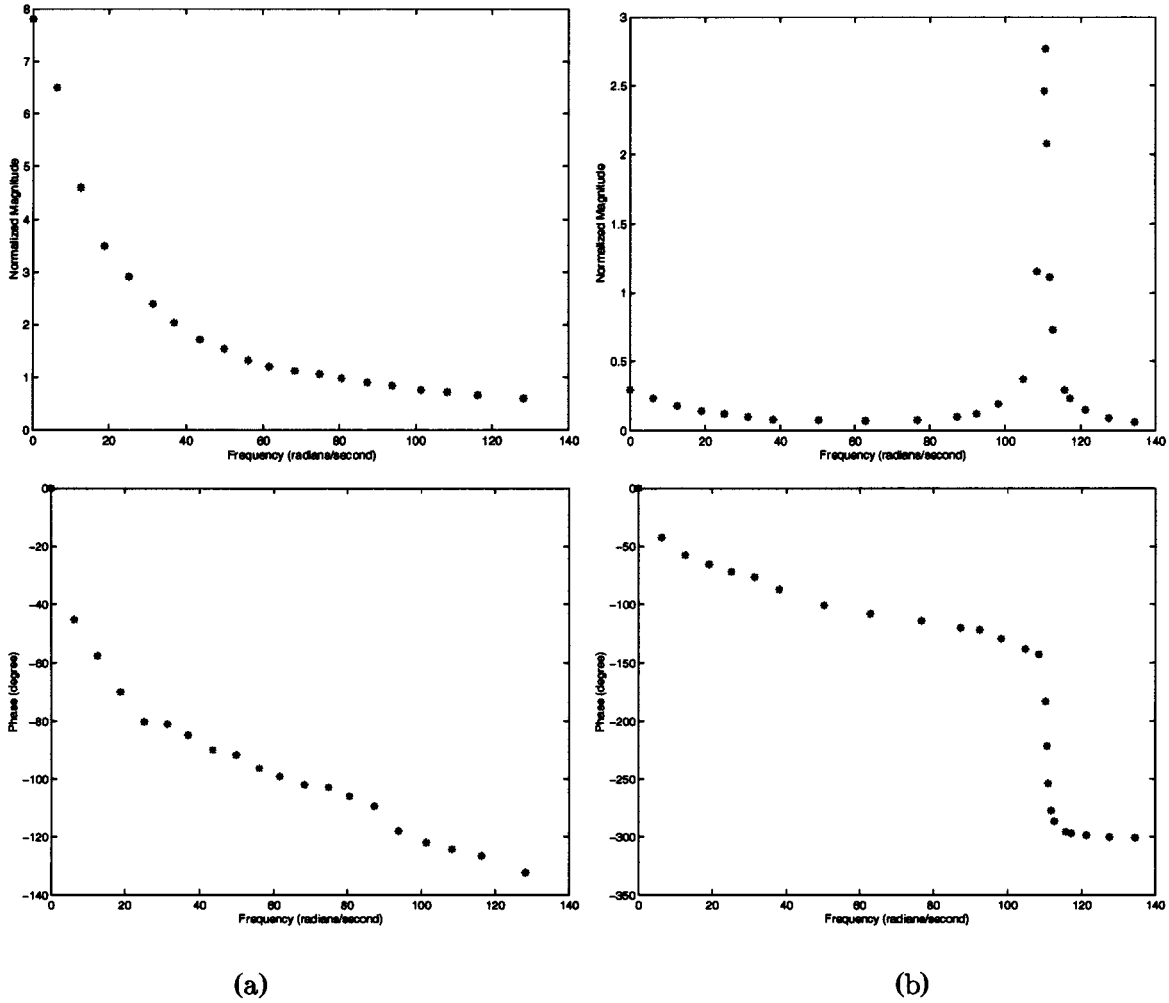

Fig. 3. Normalized experimental frequency-domain data points: (a) y_1 and (b) y_2.

to damage inducing stress, is being used to test the concepts of life-extending and damage mitigating control [16]. Life extension is achieved by designing multiobjective controllers that keep the peak values of both the time and frequency responses below some prespecified thresholds. Thus, in this application is important to have models that accurately reproduce the behavior of the system in both domains.

For benchmarking purposes the same structure is also identified using pure ℓ^1 and $\mathcal{H}_\infty$ methods, using the same total number of experimental data points (hence similar computational complexity). The quality of the resulting models is assessed by comparing their time and frequency responses against the experimental data.

A. Description of the Structure

The flexible structure used to test the proposed identification method consists of a two degree of freedom mass-beam system consisting of two discrete masses supported by cantilever beams, excited by the vibratory motion of a shaker table as shown in Fig. 1.

The first mass is connected to the shaker table, which excites the mechanical system by vibrating up and down, through a flexible pivot. The displacements y_1 and y_2 of the masses caused by the shaker table are measured using linear variable differential transformer (LVDT) sensors located at the midpoints of the masses M_1 and M_2 connected to a data-acquisition board. Thus, the problem becomes that of identifying a sampled-data system, i.e., a continuous-time system cascaded with zero order hold elements. The numerical values of the parameters are given in Table I, where L, H, W and E denote the length, height, width, and Young's modulus of each beam (see [16] for details).

An eigenvalue analysis of the model obtained using these values yields $f_1 = 9.14$ Hz and $f_2 = 17.67$ Hz for the natural frequencies of the first and second modes of vibration [16]. The first mode has large damping due to the coupling of the mass M_1 to the shaker table used as an actuator. On the other hand, the 17.67 Hz mode is very lightly damped, with a damping ratio on the order of 10^{-2}.

B. Selection of the Input Signals

Since the proposed algorithm is interpolatory, it is convergent [15, Ch. 10]. Thus, as the number of data points $N \to \infty$, the identified model converges to the actual model. However, from a practical standpoint the number of data points is limited by two factors: 1) As shown in Lemma 1 the problem becomes ill-conditioned exponentially with N and 2) the computational

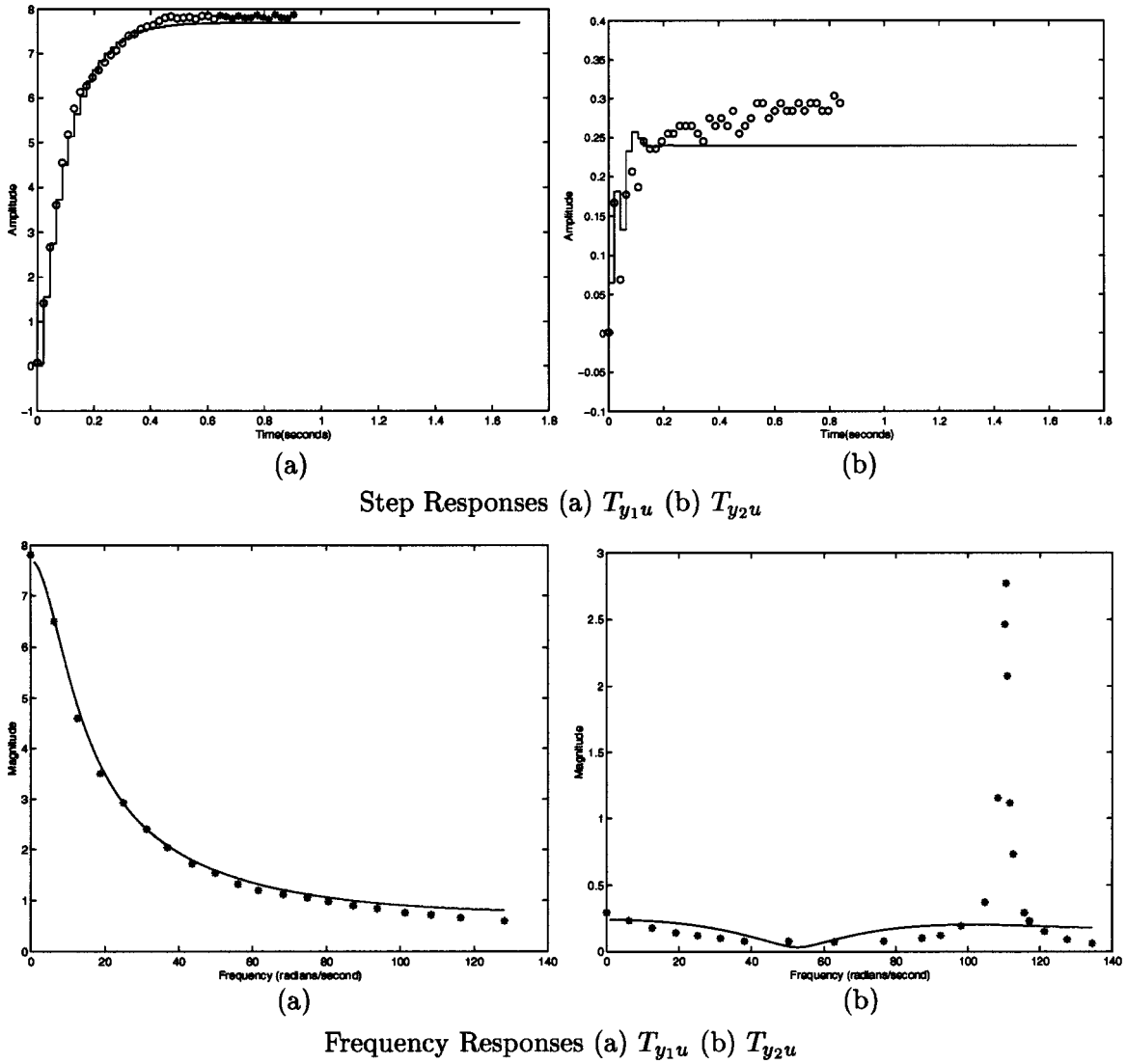

Fig. 4. Responses of the reduced order models found using ℓ_1 identification.

complexity of currently available LMI solvers grows as N^5. It can be shown that [15], for a given N, the time domain signal that yields the lowest worst-case identification error is an impulse. However, the low damping and physical constraints on the structure prevent the use of signals that approximate an impulse. As a good compromise between identification error and ease of implementability in this paper we used a step as the time-domain input. The frequency response data was obtained by driving the structure by peak-to-peak 0.5-V sinusoidal signals, with frequencies ranging from 1 Hz to 21 Hz. This frequency range captures the first two resonant modes (9 and 17.7 Hz).

C. Time-Domain Experiments

As indicated above, in principle a step input offers a compromise between physical implementability and worst case error. However, due to stiction phenomena in the actuators a single step will not yield a correct model. This was avoided by exciting the structure with a peak-to-peak 0.5-V 2 Hz square wave and collecting the data after a few cycles. By measuring the output in the absence of a driving signal it was determined that the normalized noise levels were $\epsilon_{t_1} = 0.04$ V and $\epsilon_{t_2} = 0.07$ V in y_1 and y_2, respectively. The data points (normalized by the input) are shown in Fig. 2.

D. Frequency-Domain Experiments

By measuring the output in the absence of a driving signal it was determined that in this case the (normalized) measurement noise was bounded by $\epsilon_{f_1} = 0.04$ V in y_1 and by $\epsilon_{f_2} = 0.1$ V in y_2. The frequency-domain data points, normalized by the input amplitude are shown in Fig. 3.

Following a common technique used to obtain real-rational models in Nevanlinna–Pick type identification, the complex conjugates of these points were added to set of experimental data, to obtain a set with conjugate symmetry.

IV. Identification Results

As discussed in Section II-C, the order of the central ($q = 0$) models of T_{y1u} and T_{y2u} obtained using Carathéodory–Fejér

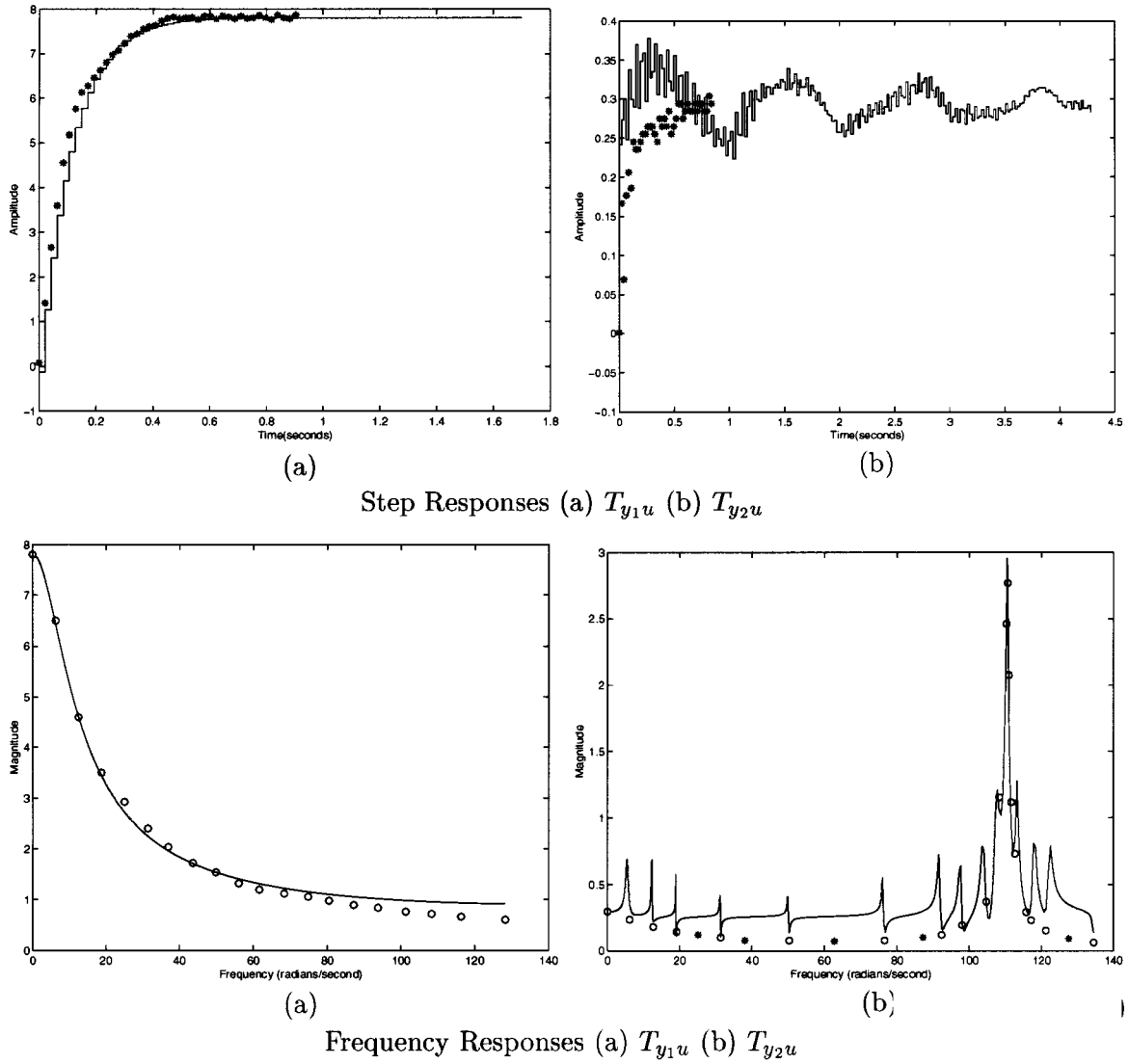

Fig. 5. Responses of the reduced order models found using $\mathcal{H}_\infty$ identification.

identification is equal to the number of time-domain data points (in this case 30 and 40, respectively). However, model reduction using balanced truncation yielded first- and third-order models of $T_{y1,\,u}$ and T_{y2u} still interpolating the time-domain data points within the error bounds and having virtually the same frequency response. Fig. 4 shows the time and frequency responses of these reduced-order model and compares them against the experimental data. In this figure "o" denotes an experimental data point used in the identification, while "$*$" denotes additional experimental data, plotted for validation purposes. As shown there, the responses of the model obtained for T_{y_1u} match well the experimental data points. On the other hand, while the step response of the identified model for T_{y_2u} matches the experimental time-domain data points within the experimental error, the frequency domain matching is rather poor, completely missing the resonance peak.

Fig. 5 shows the step and frequency responses of the first– and 30th-order models of T_{y1u} and T_{y2u} obtained after performing balanced truncation model reduction on the original 39th-order models obtained using $\mathcal{H}_\infty$-based identification. As before, the model obtained for T_{y_1u} fits both sets of experimental data-points within the error level. However, in this case the frequency response of the identified model for T_{y_2u} interpolates the experimental frequency-domain data points well, while the step response is quite different.

From these experiments it follows that either ℓ_1 and $\mathcal{H}_\infty$ identification are adequate for identifying T_{y_1u}, where the resonant peak is well damped. On the other hand, both methods fail to capture the complete behavior of T_{y_2u}.

Nonparametric mixed $\ell_1/\mathcal{H}_\infty$ identification takes into account both sources of data. Hence the corresponding model for T_{y_2u} interpolates the experimental data within the error bounds. Note however that in this case the order of the central model is given by $N = N_f + N_t = 44$. Model reduction was done using balanced realizations but even increasing the error bounds to $\epsilon_{t_2} = 0.15$ and $\epsilon_{f_2} = 0.39$ yields an 19th-order model. This is due to the fact that, when using pure nonparametric estimation, the *a posteriori* information $(K,\ \rho)$ characterizes only the smoothness and peak magnitude of the class of models, but does not include additional structural information, such as number or

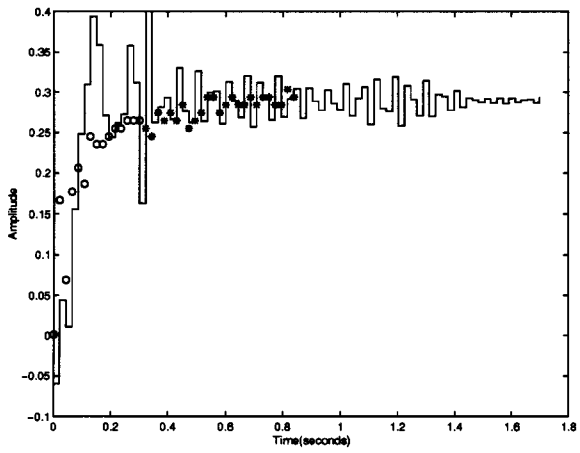

(a)

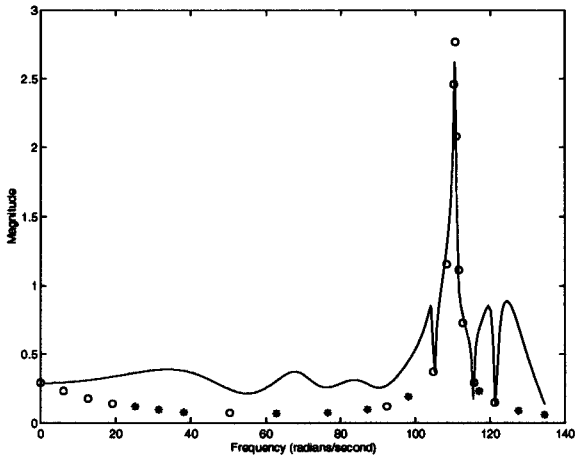

(b)

Fig. 6. Simulation results for the reduced order model of T_{y_2u} found using nonparametric mixed $\ell_1/\mathcal{H}_\infty$ identification.

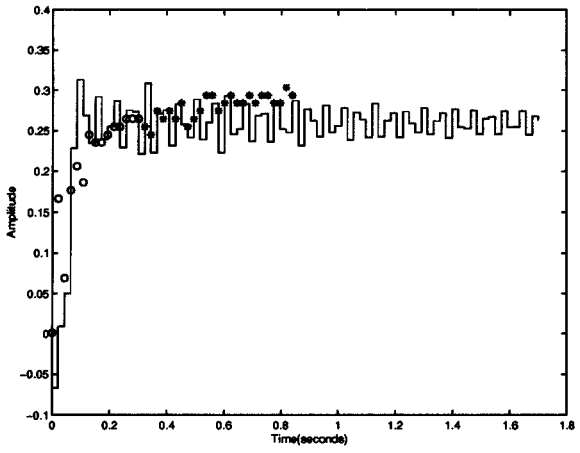

(a)

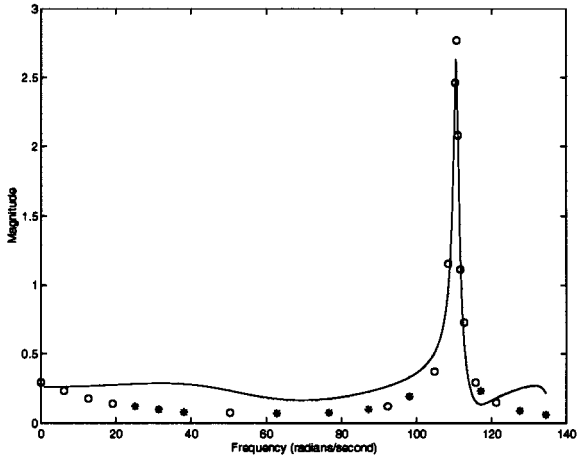

(b)

Fig. 7. Simulation results for the reduced order model found using parametric/nonparametric mixed $\ell_1/\mathcal{H}_\infty$ identification.

approximate location of resonant peaks. As illustrated in Fig. 6, this leads to conservative results in cases where the plant has large, narrow peaks in its responses, by forcing the use of very small values for ρ and large values for K.

This difficulty can be overcome by using parametric/nonparametric mixed $\ell_1/\mathcal{H}_\infty$ identification. To this effect, the resonance is handled by describing the parametric portion of the flexible structure in terms of the following second-order Kautz filters:

$$G_1(s) = \frac{p_1\sqrt{2c}s}{s^2+bs+c} \quad \text{and} \quad G_2(s) = \frac{p_2\sqrt{2bc}}{s^2+bs+c}$$
$$b = 1.211, \quad c = 1.22 \times 10^4 \tag{29}$$

where the parameter values b and c were chosen to match the information available on the critical frequencies and damping factors of the plant output y_2. Solving the LMI feasibility problem given by (6)–(8) with $\rho = 1.001$ and $K = 0.41$ yields $p_1 = -0.0215$ and $p_2 = 1.6863$. The nonparametric portion of the model can now be obtained from (22). To illustrate the potential advantages of the method over conventional approaches, in this case we used only $N_t = 15$ and $N_f = 29$ points, so that the *total* number of data points (and hence computational complexity) is similar to the pure ℓ_1 and $\mathcal{H}_\infty$ cases, obtaining a 44th-order model that interpolates the data within the experimental error levels. While the order of this model is similar to the one found using nonparametric identification (since comparable number of experimental data points were used), now it is more amenable to model reduction. In this case balanced truncation yielded a seventh-order model that interpolates well both sources of data. The responses of this reduced order model are shown in Fig. 7, where, as before "o" denotes experimental data points used in the identification and "$*$" denotes additional experimental data. A complete comparison between the models obtained using different methods is given in Table II.

V. Conclusion

In this paper we use the problem of identifying a lightly damped flexible structure, intended to explore the concept of damage-mitigating controllers [16], to benchmark several recently proposed robust identification methods. Since these controllers attempt to keep both the time and frequency domain responses of the plant below given "safety" thresholds, in this context it is important to have models that accurately replicate its behavior in both domains. As shown in Section III, due to the light damping of the plant, both the frequency and

TABLE II
IDENTIFICATION RESULTS FOR T_{y_2u}

Method:	ℓ_1	$\mathcal{H}_\infty$	Mixed (non par.)	Mixed par/non–par.
Number of data points:	40	39	15+29	15+29
Model order:	3	39	19	7
Max. error in time:				
id points only:	0.07	–	0.15	0.12
all points:	0.07	0.39	0.15	0.12
Max. error in freq:				
id points only:	–	0.056	0.39	0.33
all points:	2.92	0.54	0.74	0.33

time-domain responses exhibit peaks that lead to difficulties when using either Carathéodory–Fejér or Nevanlinna–Pick identification methods. Purely nonparametric mixed $\ell^1/\mathcal{H}_\infty$ identification can solve this problem. However, in this case the presence of lightly damped poles leads to small values of ρ and larger values of K. This in turn results in larger interpolation error bounds as well as oscillatory interpolation functions and large order models.

These difficulties can be solved by using a mixed parametric/nonparametric approach, where the resonant behavior of the plant is captured using second-order Kautz filters (with parameters to be determined) and nonparametric identification is used to identify any residual dynamics. As we show in Section IV, this approach leads to low-order models that interpolate all the experimental data points (both in the time and frequency domains) within the given error bounds.

A potential drawback shared by all the methods discussed in this paper is the computational complexity of the resulting LMI optimization problem. Since this complexity grows as N^5, these methods cannot at this point handle large amounts of experimental data. Note, however, that by exploiting time and frequency domain data in a mixed parametric/ nonparametric context, the proposed method requires a smaller amount of data points to obtain models capturing the complete behavior of the plant.

REFERENCES

[1] J. Chen, C. Nett, and M. Fan, "Worst-case system identification in $\mathcal{H}_\infty$: Validation of *a priori* information, essentially optimal algorithms, and error bounds," *Proc. Amer. Contr. Conf.*, 1992.

[2] J. Chen, J. Farrell, C. Nett, and K. Zhou, "$\mathcal{H}_\infty$ identification of multivariable systems by tangential interpolation methods," in *Proc. Conf. Decision Contr.*, 1994.

[3] J. Chen and C. Nett, "The Carathéodory-Fejér problem and the $\mathcal{H}_\infty/\ell_1$ identification: A time domain approach," *IEEE Trans. Automat. Contr.*, vol. 40, Apr. 1995.

[4] D. K. De Vries and P. M. Van Den Hof, "Quantification of uncertainty in transfer function estimation: A mixed probabilistic–worst case approach," *Automatica*, vol. 31, no. 4, pp. 543–557, 1995.

[5] G. Gu and P. Khargonekar, "A class of algorithms for identification in $\mathcal{H}_\infty$," *Automatica*, vol. 28, no. 2, 1992.

[6] J. Helmicki, C. Jacobson, and C. Nett, "Control oriented system identification: A worst case/deterministic approach in $\mathcal{H}_\infty$," *IEEE Trans. Automat. Contr.*, vol. 36, Oct. 1991.

[7] C. Jacobson, C. Nett, and J. Partington, "Worst-case system identification in ℓ_1: Optimal algorithms and error bounds," *Syst. Contr. Lett.*, vol. 19, 1992.

[8] L. Giarré and M. Milanese, "Model quality evaluation in $\mathcal{H}_2$ identification," *IEEE Trans. Automat. Contr.*, vol. 42, no. 5, pp. 691–698, 1997.

[9] P. Mäkilä, "Robust identification and Galois sequences," *Int. J. Contr.*, vol. 54, no. 5, 1991.

[10] M. Milanese, "Worst-case ℓ_1 identification," in *Bounding Approaches to System Identification*, Piet-Lahanier and Walter, Eds. New York: Plenum, 1994.

[11] P. Parrilo, M. Sznaier, R. S. Peña, and T. Inanc, "Mixed time/frequency domain robust identification," *Automatica*, vol. 34, no. 11, pp. 1375–1389, Nov. 1998.

[12] P. Heuberger, P. Van den Hof, and O. Bosgra, "A generalized orthonormal basis for linear dynamical systems," *IEEE Trans. Automat. Contr.*, vol. 40, Mar. 1995.

[13] P. A. Parrilo, R. S. Peña, and M. Sznaier, "A parametric extension of mixed time/frequency robust identification," *IEEE Trans. Automat. Contr.*, vol. 44, pp. 364–369, Feb. 1999.

[14] J. Partington, "Robust Identification in $\mathcal{H}_\infty$," *J. Math. Anal. Applicat.*, vol. 166, pp. 428–441, 1992.

[15] R. S. Pena and M. Sznaier, *Robust Systems Theory and Applications*, 1998.

[16] S. Tangirala, M. Holmes, A. Ray, and M. Carpino, "Life-extending control of mechanical structures: Experimental verification of the concept.," *Automatica*, vol. 34, no. 1, pp. 3–14, 1998.

[17] T. Zhou and H. Kimura, "Time domain identification for robust control," *Syst. Contr. Lett.*, vol. 20, pp. 167–178, 1993.

Tamer Inanc was born in 1970 in Izmir, Turkey. He received the Bachelor of Science degree in electrical engineering from Dokuz Eylul University, Izmir, Turkey, in 1991. In 1993, he won a merit scholarship award given by Government of Turkey the M.S. and Ph.D. degrees. He completed the M.S. degree in electrical engineering from Pennsylvania State University, University Park, in 1996. His M.S. thesis was titled as "Mixed $\ell_1/\mathcal{H}_\infty$ Robust Identification: Application to a Flexible Structure Testbed." He is currently pursuing the Ph.D. degree at the same university. His dissertation focuses on finding a novel approach to model active vision systems without any need of calibration and to design a controller which guarantees stability of an active vision system under changing zoom values.

His research interetst include robust control, robust identification, active vision systems, computer vision, and image processing.

Mario Sznaier (S'89–M'89) received the Ingeniero Electronico and Ingeniero en Sistemas de Computacion degrees from the Universidad de la Republica, Uruguay, in 1983 and 1984, respectively, and the M.S.E.E. and Ph.D. degrees from the University of Washington, Seattle, in 1986 and 1989, respectively. From 1991 to 1993 he was an Assistant Professor of Electrical Engineering at the University of Central Florida.

In 1993, he joined the Department of Electrical Engineering at the Pennsylvania State University, University Park, where he is currently an Associate Professor. He was also Visiting Research Fellow in Electrical Engineering in 1990 and Visiting Associate Professor of Control and Dynamical Systems in 2000 to 2001 with the California Institute of Technology, Pasadena. His research interest include multiobjective robust control; ℓ_1 and $\mathcal{H}_\infty$ control theory, control oriented identification, and active vision.

Pablo A. Parrilo was born in Buenos Aires, Argentina. He received the Electronics Engineering degree from the University of Buenos Aires in 1994 and the Ph.D. degree in control and dynamical systems from the California Institute of Technology, Pasadena, in June 2000.

He is currently a Postdoctoral Scholar at Caltech. His research interests include robust control and identification and general robustness analysis.

Ricardo S. Sánchez Peña (S'86–M'89–SM'00) was born in Mendoza, Argentina, in 1954. He received the Ingeniero en Electrónica degree from the University of Buenos Aires in 1978 and the M.S. and Ph.D. in electrical engineering from the California Institute of Technology, Pasadena, in 1986 and 1988, respectively.

He has worked for several Research Institutions in Argentina (CITEFA, CNIE, CNEA) and Germany (DLR) since 1977. He is currently a Researcher at the National Commission of Space Activities (CONAE) where he collaborated in the design of the first 3 argentine satellites and coordinates the area of NG&C. He is also Professor of the Electrical Engineering Department at the University of Buenos Aires and Director of the Identification and Robust Control Group (GICOR). His research interests are in the applications of robust identification and control to practical problems. He is the author of *Introducción a la Teoria de Control Robusto* (AADECA, 1992), winner of the 1991 book contest organized by the Argentine IFAC representative, and coauthor of *Robust Systems Theory and Applications* (New York: Wiley, 1998) and the Robust Systems chapter in the *Electrical Engineering Handbook* (Boca Raton, FL: CRC, 2000). He is Process Control Editor of the journal *Latin American Applied Research* and has authored more than 70 journal and conference papers.